JCAMECH
Vol. 46, No. 2, July 2015, pp 191- 204

Transient thermo-visco-elastic response of a functionally graded non-axisymmetric cylinder

Rahmatollah Ghajar[1*], Mahmood M. Shokrieh[2] and Ali R. Shajari[1]

1. Mechanical Properties Research Lab (MPRL), Faculty of Mechanical Engineering, K.N. Toosi Univeristy of Technology, Iran

2. Composites Research Laboratory, Center of Excellence in Experimental Solid Mechanics and Dynamics, School of Mechanical Engineering, Iran University of Science and Technology, Iran

Received: May 24, 2015; Accepted: July 12, 2015

Abstract

In this study, the analysis of transient thermoelastic response of a functionally graded (FG) non-axisymmetric viscoelastic cylinder is presented. The material properties are assumed to be time-dependent and radially and circumferentially non-homogeneous. The finite element (FE) formulations of the thermoelastic problem are obtained using the virtual work method and all the coupling terms are considered. According to material dependencies and nonlinearity of the constitutive equation, an iterative-based FE solution is suggested in order to solve thermo-elastic equations. The effects of material in homogeneities on the time-dependent response of mechanical and thermal components are investigated. From the results of this study, it is concluded that, using appropriate material inhomogeneities can improve the magnitudes of stress components, especially shear stress.

Keywords: *finite element method, functionally graded material, non-axisymmetric, transient thermoelasticity, viscoelastic.*

1. Introduction

The thermoelastic analysis of different structures such as cylinders, disks, shafts among others have attracted much attention among researchers due to their applications in various industries. The analyses of thick-walled cylindrical vessels under thermal and mechanical loads have been widely studied, considering some assumption including plane strain and symmetry about axis [1-3]. In many applications, the mentioned assumptions cannot be taken into account [4, 5]. For example, in a cylinder under hydrostatic pressure, the magnitude of pressure changes longitudinally, therefore the plane strain condition is not valid [6].

For the cases of cylindrical vessels under non-axisymmetric loads, shear stress component is created which decreases the lifetime of cylinders. The analysis of thermoelastic

∗ Corresponding Author, Tel: +98 21 84063240
Email: ghajar@kntu.ac.ir

response of cylinders under non-axisymmetric thermal field was performed by Takeuti and Noda [7]. They solved uncoupled transient thermoelastic equations for an isotropic finite cylinder analytically.

For the special purposes, functional graded (FG) materials have been used in some industries to endure high thermal stresses. The general solution for mechanical and thermal stresses in a FG cylinder under steady state non-axisymmetric loads was presented by Jabbari et al. [8]. They assumed a power-low function for the FG material and used the separation of variables and complex Fourier series to solve thermoelastic governing equations. Tokovyy and Ma [9] presented an analysis of 2D non-axisymmetric elastic and steady state thermoelastic of FG cylinders. They assumed the cylinder to be radially inhomogeneous and used the Vihak method which is based on the integration of the original differential equilibrium equations, independent of the stress–strain relations. They implemented the mentioned method for various inhomogeneous annular domains [10]. As a different study about non-axisymmetric FG cylinders, Li and Liu [11] analyzed the elastic behavior of a radially inhomogeneous hollow cylinder under non-axisymmetric arbitrary load using complex potential stress functions. The major shear stress with respect to other stress components was observed in their results.

Transient thermoelastic analysis of structures due to dynamic loadings or time-dependent constitutive equations of the materials has been considered in many studies.. Coupled dynamic thermoelastic response of a thin-walled plate under thermal and mechanical shock loadings were analyzed by Zheng et al. [12]. They used a novel meshless local Petrov-Galerkin approach and backward difference time iteration to solve motion and heat equations, simultaneously. Their results showed that the values of stress components are increased remarkably under thermal shock with respect to steady state thermoelastic condition. In addition to dynamic loading cases, transient thermoelastic problems are important for materials with time-dependent structural properties. One of the most important materials with structural time-dependency is viscoelastic material.

Viscoelastic properties have been found in many materials such as polymers and high temperature metals. The time-dependent constitute equations of these materials have profound effects on their elastic and thermoelastic responses especially in dynamic and transient problems. Applications of viscoelastic materials as the FG material have been studied in recent years [13-16].

Temel et al. [17] presented the analysis of elastic and viscoelastic responses of radially inhomogeneous annular structures. They used Laplace transform to obtain a time-independent form of boundary-value problem in terms of spatial coordinates. The results were converted to primary time domain using the modified Durbin method.

To the best of the present authors' knowledge, circumferential inhomogeneity has not been considered so far for FG materials. Hence, in this research, a radially and circumferentially inhomogeneous viscoelastic material is considered and using an FE method, a transient thermoelastic problem for a non-axisymmetric viscoelastic FG cylinder is studied. To obtain FE formulations, the principle of virtual work is applied for equations of motion and energy balance. The thermal boundary conditions are assumed to be non-axisymmetric as a case-study and the results are presented for different times and material inhomogeneities. The results show that shear stress in the cylinder can be reduced and controlled by applying an appropriate material inhomogeneity.

2. Material constitutive equation

The constitutive equation of viscoelastic materials is demonstrated by the well-known hereditary integral as follows [18]:

$$\boldsymbol{\sigma}(t)=\mathbf{C}(0)\boldsymbol{\varepsilon}(t)-\int_0^t \frac{\partial \mathbf{C}(\tau)}{\partial \tau}\boldsymbol{\varepsilon}(t-\tau)d\tau \qquad (1)$$

where $\sigma(t)$ and $\varepsilon(t)$ are history of stress and strain tensors, respectively, $C(t)$ is relaxation stiffness and t denotes time.

For a long cylinder, the plane strain condition can be assumed that the stress and strain tensors in polar coordinates are reduced to:

$$\begin{aligned}\boldsymbol{\sigma}&=\begin{bmatrix}\sigma_{rr} & \sigma_{\theta\theta} & \sigma_{r\theta}\end{bmatrix}^T\\ \boldsymbol{\varepsilon}&=\begin{bmatrix}\varepsilon_{rr} & \varepsilon_{\theta\theta} & \gamma_{r\theta}\end{bmatrix}^T\end{aligned} \qquad (2)$$

where superscript T denotes transpose.

The stiffness tensor, with respect to isotropic viscoelastic FG properties can be written as:

$$\mathbf{C}(r,\theta,t)= \frac{E(r,\theta,t)}{(1+\nu)(1-2\nu)}\begin{bmatrix} 1-\nu & \nu & 0 \\ \nu & 1-\nu & 0 \\ 0 & 0 & (1-2\nu)/2 \end{bmatrix} \quad (3)$$

where E and ν are unidirectional relaxation modulus and the Poisson's ratio, respectively. According to the generalized Maxwell model [18] for viscoelastic materials, the relaxation modulus in terms of time is expressed as:

$$E(t)=\sum_{i=1}^{N_{PS}} E_i \exp-\frac{t}{\tau_i} \quad (4)$$

Equation (4) is known as Prony series in which E_i, τ_i and N_{PS} are elastic modulus in ith term of the series, relaxation time parameter and number of the series terms, respectively.

On the other hand, in this research, all mechanical and thermal properties of the structure are assumed to be dependent on the radial and circumferential coordinates (r, θ) as:

$$P(r,\theta)=P_0 r^m\left(1+n\sin\frac{\theta}{2}\right) \quad (5)$$

where P_0 is the value of the property inhomogeneous material and m and n are radial and circumferential material inhomogeneity indices, respectively.

It is worth mentioning that, in many thermoelastic problems, temperature dependency of the material is taken into account. However, for polymers under glass transition temperature, the structural properties are assumed to be independent of temperature [19, 20]. The temperature of the system in this study will be chosen to be below the glass transition temperature of the polymer. Hence, it is evident to say that the effect of temperature on structural properties of the material in this study is negligible.

The strain tensor can be divided into mechanical and thermal parts as follows:

$$\boldsymbol{\varepsilon}=\boldsymbol{\varepsilon}^M+\boldsymbol{\varepsilon}^T \quad (6)$$

in which

$$\boldsymbol{\varepsilon}^M=\begin{bmatrix}\varepsilon_{rr}^M & \varepsilon_{\theta\theta}^M & \gamma_{r\theta}^M\end{bmatrix}^T= \begin{bmatrix}\frac{\partial u_r}{\partial r} & \frac{1}{r}\left(u_r+\frac{\partial u_\theta}{\partial\theta}\right) & \frac{1}{r}\frac{\partial u_r}{\partial\theta}+\frac{\partial u_\theta}{\partial r}-\frac{u_\theta}{r}\end{bmatrix} \quad (7)$$

$$\boldsymbol{\varepsilon}^T=-(1+\nu)\alpha\Theta\begin{bmatrix}1 & 1 & 0\end{bmatrix}$$

In Equation (7), u_r and u_θ are radial and circumferential components of displacement, α is coefficient of thermal expansion and θ is temperature change with respect to the reference temperature T_0.

3. Formulations

In this section, the comprehensive FE formulations are derived for a general thermoelastic problem, implementing the principle of virtual work. In the process of the FE method, each element can be considered as homogenous with constant properties.

3.1. Thermoelasticity

Thermoelasticity problem in general, have two sets of equations; equations of motion and energy balance. These equations are [21]:

$$\begin{aligned}&\sigma_{ij,j}+F_i=\rho\ddot{u}_i \\ &q_{i,i}+\rho c\dot{\Theta}+\beta T_0\dot{u}_{i,i}=R\end{aligned} \quad (8)$$

where σ_{ij}, F_i, u_i and q_i are components of stress tensor, body force vector, displacement vector and heat flux vector, respectively; ρ, c, R and β are density, thermal capacity, internal heat generation, and thermal modulus which is defined as: $\beta=\frac{E(t)(1+5\nu)\alpha}{(1+\nu)(1-2\nu)}$), respectively. In Equation (8) comma, over-dot and over-double-dot denote derivation with respect to ith coordinate, first and second order time derivatives, respectively.

3.2. Principle of virtual work

According to the principle of virtual work, work done by forces due to virtual displacements on a structure in equilibrium state is zero [6]. In the FE thermoelasticity formulations, the principle of virtual work is implemented on the equations of motion and energy balance throughout the volume of an arbitrary element. It can be stated as:

$$\iiint_\Omega\left(\sigma_{ij,j}+F_i-\rho\ddot{u}_i\right)\delta u_i\, d\Omega=0 \quad (9)$$

where δu_i, $\delta\Theta$ are components of virtual displacement vector and temperature change, respectively and Ω denotes volume of the element.

By applying the Divergence theorem, Equation (9) yields:

$$\iint_{\Gamma} T_i \delta u_i d\Gamma - \iiint_{\Omega} \sigma_{ij} \delta u_{i,j} d\Omega + \iiint_{\Omega} F_i \delta u_i d\Omega - \iiint_{\Omega} \rho \ddot{u}_i \delta u_i d\Omega = 0$$
$$\iint_{\Gamma} Q \delta\Theta d\Gamma - \iiint_{\Omega} q_i \delta\Theta_{,i} d\Omega + \iiint_{\Omega} \rho c \dot{\Theta} \delta\Theta d\Omega + \iiint_{\Omega} \beta T_0 \dot{\mu}_{i,i} \delta\Theta d\Omega - \iiint_{\Omega} R \delta\Theta d\Omega = 0 \quad (10)$$

In Equation (10), T_i and Q are traction vector components and heat flux on the boundary surface of element Γ.

Finally, the tensorial form of Equation (10) for a general thermoelasticity problem can be written as:

$$\iiint_{\Omega} \delta\varepsilon^T \sigma d\Omega + \iiint_{\Omega} \rho \delta \mathrm{u}^T \ddot{\mathrm{u}} d\Omega = \iint_{\Gamma} \delta \mathrm{u}^T \mathrm{T} d\Gamma + \iiint_{\Omega} \delta \mathrm{u}^T \mathrm{F} d\Omega$$
$$-\iiint_{\Omega} (\nabla \delta\Theta)^T \mathrm{q} d\Omega + \iiint_{\Omega} \rho c \dot{\Theta} \delta\Theta d\Omega + \iiint_{\Omega} \beta T_0 (\nabla . \dot{\mathrm{u}}) \delta\Theta d\Omega = -\iint_{\Gamma} Q \delta\Theta d\Gamma + \iiint_{\Omega} R \delta\Theta d\Omega \quad (11)$$

For a non-axisymmetric long cylinder with plane strain condition, the above formulations must be converted in polar coordinates (r,θ). The field variables in this problem are components of radial and circumferential displacement (u_r,u_θ) and temperature change θ, which can be presented by vector $\boldsymbol{\phi}$ as follows:

$$\phi = \begin{bmatrix} u_r & u_\theta & \Theta \end{bmatrix}^T \quad (12)$$

Hence, the nodal values vector of the filed variables in an arbitrary element with z nodes is defined as:

$$\boldsymbol{\alpha}^e = \begin{bmatrix} u_r^1 & u_\theta^1 & \Theta^1 & \cdots & u_r^z & u_\theta^z & \Theta^z \end{bmatrix}^T \quad (13)$$

The vector of field variables ϕ, can be evaluated in terms of vector of nodal values $\boldsymbol{\alpha}^e$ by means of approximation shape functions as follows:

$$\phi_i = \sum_{j=1}^{3z} \psi_{ij} \alpha_j^e, \phi = \boldsymbol{\psi} \boldsymbol{\alpha}^e \quad (14)$$

where ψ is the matrix of the approximation shape functions.

For convenience, the following matrices are defined to express some parameters used in Equation (11), in terms of nodal values vector $\boldsymbol{\alpha}^e$:

$$\begin{aligned} \mathbf{u} &= \mathfrak{B}_1 \boldsymbol{\alpha}^e \\ \Theta &= \mathfrak{B}_2 \boldsymbol{\alpha}^e \\ \nabla\Theta &= \mathfrak{B}_3 \boldsymbol{\alpha}^e \\ \nabla.\mathbf{u} &= \mathfrak{B}_4 \boldsymbol{\alpha}^e \\ \boldsymbol{\varepsilon} &= \mathfrak{B}_5 \boldsymbol{\alpha}^e \end{aligned} \quad (15)$$

where the parameters $\mathfrak{B}_1$ to $\mathfrak{B}_5$ are

$$\begin{aligned} \mathfrak{B}_1 &= \begin{bmatrix} 1 & 0 & 0 \\ 0 & 1 & 0 \end{bmatrix} \boldsymbol{\psi} \\ \mathfrak{B}_2 &= \begin{bmatrix} 0 & 0 & 1 \end{bmatrix} \boldsymbol{\psi} \\ \mathfrak{B}_3 &= \begin{bmatrix} 0 & 0 & \partial/\partial r \\ 0 & 0 & \partial/r\partial\theta \end{bmatrix} \boldsymbol{\psi} \\ \mathfrak{B}_4 &= \begin{bmatrix} 1/r + \partial/\partial r & \partial/r\partial\theta & 0 \end{bmatrix} \boldsymbol{\psi} \\ \mathfrak{B}_5 &= \begin{bmatrix} \partial/\partial r & 0 & -(1+\nu)\alpha \\ 1/r & \partial/\partial\theta & -(1+\nu)\alpha \\ \partial/r\partial\theta & \partial/\partial r - 1/r & 0 \end{bmatrix} \boldsymbol{\psi} \end{aligned} \quad (16)$$

Substituting Equation (15) in Equation (11), yields:

$$\iiint_{\Omega} \mathfrak{B}_5^T \boldsymbol{\sigma} d\Omega + \iiint_{\Omega} \rho \mathfrak{B}_1^T \mathfrak{B}_1 \ddot{\boldsymbol{\alpha}}^e d\Omega = \iint_{\Gamma} \mathfrak{B}_1^T \mathbf{T} d\Gamma + \iiint_{\Omega} \mathfrak{B}_1^T \mathbf{F} d\Omega$$
$$-\iiint_{\Omega} \mathfrak{B}_3^T \mathbf{q} d\Omega + \iiint_{\Omega} \rho c \mathfrak{B}_2^T \mathfrak{B}_2 \dot{\boldsymbol{\alpha}}^e d\Omega + \iiint_{\Omega} \beta T_0 \mathfrak{B}_2^T \mathfrak{B}_4 \dot{\boldsymbol{\alpha}}^e d\Omega = -\iint_{\Gamma} Q \mathfrak{B}_2^T d\Gamma + \iiint_{\Omega} R \mathfrak{B}_2^T d\Omega \quad (17)$$

Considering heat conduction and no heat generation in the cylinder, the vector of heat flux can be written in terms of temperature change Θ and conductivity k, as follows [21]:

$$\mathbf{q} = -k \nabla\Theta \quad (18)$$

Substituting Equation (18) and hereditary constitutive equations of the material (Eq. 1) in Equation (17), the dynamics of FE formulations of the problem are obtained as:

$$\begin{aligned}&\iiint_\Omega \mathfrak{B}_5^T C(0)\mathfrak{B}_5\mathbf{a}^e d\Omega - \iiint_\Omega \mathfrak{B}_5^T\left[\int_0^t \dot{\mathbf{C}}(\tau)\mathfrak{B}_5\dot{\mathbf{a}}^e(t-\tau)d\tau\right]d\Omega + \iiint_\Omega \rho\mathfrak{B}_1^T\mathfrak{B}_1\ddot{\mathbf{a}}^e d\Omega = \iint_\Gamma \mathfrak{B}_1^T\mathbf{T}d\Gamma + \iiint_\Omega \mathfrak{B}_1^T\mathbf{F}d\Omega\\ &\iiint_\Omega k\,\mathfrak{B}_3^T\mathfrak{B}_3\mathbf{a}^e d\Omega + \iiint_\Omega \rho c\,\mathfrak{B}_2^T\mathfrak{B}_2\dot{\mathbf{a}}^e d\Omega + \iiint_\Omega \beta T_0\mathfrak{B}_2^T\mathfrak{B}_4\dot{\mathbf{a}}^e d\Omega = -\iint_\Gamma Q\mathfrak{B}_2^T d\Gamma + \iiint_\Omega R\,\mathfrak{B}_2^T d\Omega\end{aligned} \tag{19}$$

These formulations can be reduced as follows:

$$\mathbf{M}\ddot{\mathbf{a}}^e + \mathbf{D}\dot{\mathbf{a}}^e + \mathbf{K}\mathbf{a}^e + \bar{\mathbf{K}}(t) = \mathbf{f} \tag{20}$$

where M represents the mass, D damping and K stiffness and their matrices are thus:

$$\begin{aligned}\mathbf{M} &= \iiint_\Omega \rho\mathfrak{B}_1^T\mathfrak{B}_1 d\Omega\\ \mathbf{D} &= \iiint_\Omega \left(\rho c\,\mathfrak{B}_2^T\mathfrak{B}_2 + \beta T_0\mathfrak{B}_2^T\mathfrak{B}_4\right)d\Omega\\ \mathbf{K} &= \iiint_\Omega \left[\mathfrak{B}_5^T C(0)\mathfrak{B}_5 + k\,\mathfrak{B}_3^T\mathfrak{B}_3\right]d\Omega\end{aligned} \tag{21}$$

and time-dependent stiffness due to the viscoelasticity of the material is expressed as:

$$\bar{\mathbf{K}}(t) = -\iiint_\Omega \mathfrak{B}_5^T\left[\int_0^t \dot{\mathbf{C}}(\tau)\mathfrak{B}_5\dot{\mathbf{a}}^e(t-\tau)d\tau\right]d\Omega \tag{22}$$

The force vector f in Equation (19) is obtained as:

$$\begin{aligned}\mathbf{f} = &\iint_\Gamma \boldsymbol{\psi}^T\begin{bmatrix}T_r & T_\theta & -Q\end{bmatrix}^T d\Gamma +\\ &\iiint_\Omega \boldsymbol{\psi}^T\begin{bmatrix}F_r & F_\theta & R\end{bmatrix}^T d\Omega\end{aligned} \tag{23}$$

The natural boundary conditions of the structure including internal and external pressure and heat flux are taken into account in the first term of force vector.

The form of the shape functions depends on the element configurations. In this study, a second order quadratic element, shown in Figure 1, is chosen. The shape functions of this element are as follows:

$$\boldsymbol{\psi} = \begin{bmatrix}\mathcal{N}_1 & 0 & 0 & \cdots & \mathcal{N}_\xi & 0 & 0\\ 0 & \mathcal{N}_1 & 0 & \cdots & 0 & \mathcal{N}_\xi & 0\\ 0 & 0 & \mathcal{N}_1 & & 0 & 0 & \mathcal{N}_\xi\end{bmatrix} \tag{24}$$

where

$$\begin{aligned}&\mathcal{N}_1 = (1+\zeta)(1-\xi)(\zeta-\xi-1)/4, \quad \mathcal{N}_5 = (1+\zeta)(1-\xi^2)/2\\ &\mathcal{N}_2 = (1+\zeta)(1+\xi)(\zeta+\xi-1)/4, \quad \mathcal{N}_6 = (1+\xi)(1-\zeta^2)/2\\ &\mathcal{N}_3 = (1-\zeta)(1+\xi)(-\zeta+\xi-1)/4, \quad \mathcal{N}_7 = (1-\zeta)(1-\xi^2)/2\\ &\mathcal{N}_4 = (1-\zeta)(1-\xi)(-\zeta-\xi-1)/4, \quad \mathcal{N}_8 = (1-\xi)(1-\zeta^2)/2\\ &-1\le\zeta,\xi\le+1\end{aligned} \tag{25}$$

in which, ζ and ξ are local coordinates as shown in Figure 1.

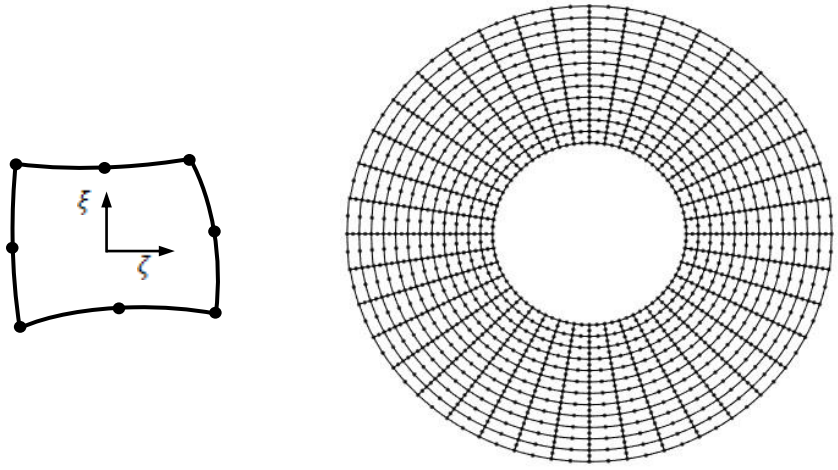

(a) (b)

Fig. 1. a) Local coordinates of quadratic brick solid element, b) Meshing of problem domain

3.3. Solution procedure

Equation (20) is a set of nonlinear differential equations which cannot be solved explicitly due to the existence of term $\bar{\mathbf{K}}(t)$. Hence, an iterative-based incremental method is proposed according to the following steps:

Step 1: Neglect $\bar{\mathbf{K}}(t)$, solve Equation (20) and obtain nodal values of field variables $\mathbf{a}^e$. To solve the equations without considering $\bar{\mathbf{K}}(t)$, the Laplace transform is applied as

$$\mathbf{M}\left[s^2\boldsymbol{\mathcal{A}}^e - s\mathbf{a}^e(0) - \dot{\mathbf{a}}^e(0)\right] + \mathbf{D}\left[s\boldsymbol{\mathcal{A}}^e - \mathbf{a}^e(0)\right] + \mathbf{K}\boldsymbol{\mathcal{A}}^e = \mathbf{f} \tag{26}$$

where $A^e = L\left\{a^e\right\}$. Regarding zero initial conditions, the vector of nodal values are calculated as

$$\mathbf{a}^e = \mathcal{L}^{-1}\left\{\left[\mathbf{M}s^2 + \mathbf{D}s + \mathbf{K}\right]^{-1}\mathbf{f}\right\} \tag{27}$$

Step 2: Evaluate $\bar{\mathbf{K}}(t)$ using values obtained from the previous step.

Step 3: Solve Equation (20), considering $\bar{\mathbf{K}}(t)$ of the previous step and obtain new a^e.

Step 4: Compare old a^e with updated ones, if convergence is not achieved, steps 2 to 4 must be repeated.

The above procedure is performed until the maximum relative error between two successive iterations becomes less than a certain value such as 0.1%.

4. Numerical results and discussion

In this study, a cylindrical pressure vessel with 0.2 and 0.5 m as inner and outer radii, respectively, made of poly methyl methacrylate (PMMA) is considered. The thermal and relaxation properties of the PMMA are shown in Table 1 [22, 23].

Table 1. Material properties of PMMA [22 - 23]

Relaxation parameters			Thermal	Density	Poisson's ratio
i	E_i (GPa)	τ_i (sec)	$c = 1466\left(\frac{\mathrm{J}}{\mathrm{K\,kg}}\right)$	$\rho = 1180\left(\frac{\mathrm{kg}}{\mathrm{m}^3}\right)$	$\nu = 0.44$
0	1.419	0			
1	0.298	9.1955e-1	$\alpha = 70\times10^{-6}\left(\frac{1}{\mathrm{K}}\right)$		
2	0.064	9.8120e0			
3	0.158	9.5268e1	$k = 0.2\left(\frac{\mathrm{W}}{\mathrm{m\,K}}\right)$		
4	0.181	9.4318e2			
5	0.239	9.2066e3			
6	0.278	8.9974e4			
7	0.328	8.6852e5			
8	0.323	8.5143e6			
9	0.405	7.7396e7			

As mentioned in section 2, the temperature of the system must be under glass transition temperature of the material. The glass transition temperature of the PMMA is reported by Ashby [24] as 100-165°C. Therefore, the following internal and external pressures, with non-axisymmetric thermal loads are applied on the cylinder as:

$$P_i = 100\mathrm{MPa}, P_o = 10\mathrm{MPa}$$
$$T_i = 400\mathrm{K}, T_o = 300\left(1 + 0.3\sin\sin\frac{\theta}{2}\right)\mathrm{K} \tag{28}$$

The thermal boundary conditions are schematically illustrated in Figure 2.

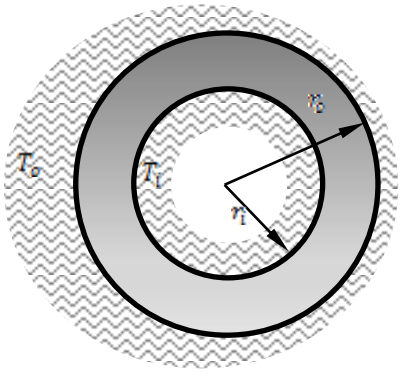

Fig. 2. Functionally graded viscoelastic cylinder under non-axisymmetric thermal boundary conditions

The initial conditions of the structure are

$$u_r(r,\theta,0)=u_\theta(r,\theta,0)=0$$
$$\dot{u}_r(r,\theta,0)=\dot{u}_\theta(r,\theta,0)=0 \qquad (29)$$
$$T(r,\theta,0)=T_0 \rightarrow \Theta(r,\theta,0)=0$$

In time-dependent FE problems, results must be independent of mesh size and time increment. Tables 2 and 3 present the radial displacement in point $(r,\theta)=(0.35,0)$ for different number of elements and time increments, respectively. It is observed that using 12 radial and 40 circumferential elements with time increment $\Delta t = 1e-5\,\text{sec}$ gives adequate convergent results.

Table 2. Results dependency to the number of elements

Number of elements		$u_r(0.35,0,100)$
Radial	Circumferential	
8	20	0.0040
12	20	0.0041
16	20	0.0044
8	30	0.0044
12	30	0.0049
16	30	0.0048
8	40	0.0051
12	40	0.0050
16	40	0.0050
8	50	0.0050
12	50	0.0050
16	50	0.0050

Table 3. Results dependency to the time incitement

Δt	$u_r(0.35,0,1e3)$	$u_r(0.35,0,1e4)$
1e-2	0.00626	0.00702
1e-3	0.00622	0.00690
1e-4	0.00610	0.00691
1e-5	0.00603	0.00691
1e-6	0.00602	0.00691

4.1. Time-dependent responses of homogeneous cylinder

The time dependent responses of parameters including temperature change, radial displacement and stress components were also described. The radial distributions of the mentioned parameters at different times in two directions θ=0 and 180, and a 3D distribution of parameters at 1e4 sec were shown and discussed.

Figure 3 (a) shows the radial variation of temperature change θ during the time. It is observed that temperature distribution becomes smoother with time. As mentioned in Equation (25), the outer temperature of the cylinder is varied along the circumference. Therefore, the distribution of θ for two directions $\theta=0$ and 180 become considerably different near the outer radius at every time. Figure 3(b) shows in three dimensions, the radial and circumferential variation in temperature change is shown three dimensionally.

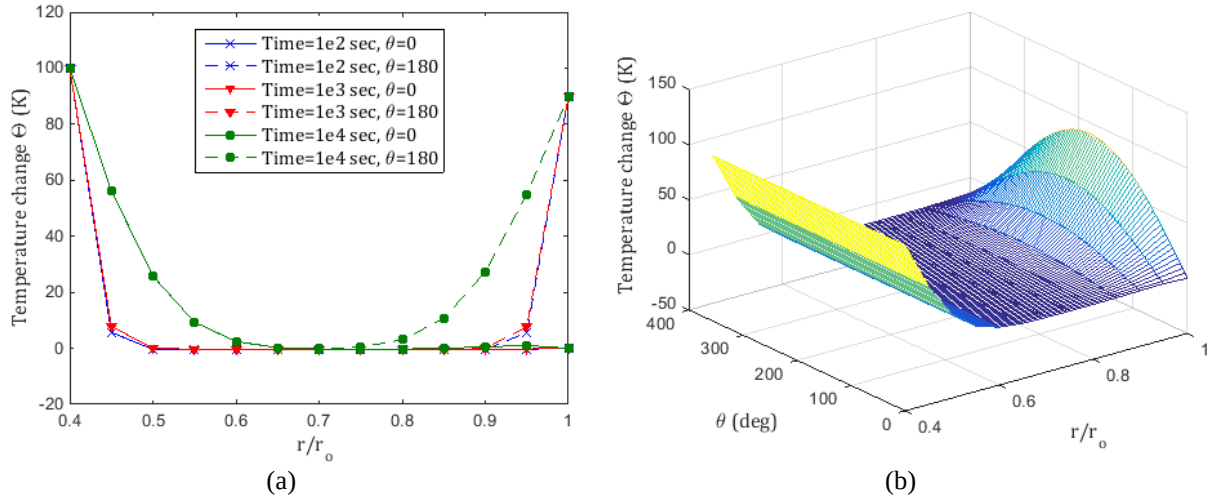

(a) (b)

Fig. 3. a) Radial distribution of temperature change for different times and directions, b) 3-D distribution of the temperature change for time 1e4 sec

The variations in radial displacement along the radius at different times and a 3-D distribution of u_i in time 1e4 sec are illustrated in Figure 4. As can be seen from this figure, maximum displacement is observed in the inner surface for any condition. In addition, it is observed that by increasing the time, magnitudes of radial displacement are increased. It can also be observed that the difference between values in directions θ=0 and 180 become remarkable with time.

Figure 5 presents radial stress variation along the radius. A small change can be observed for radial stress by changing time and directions. From Figure 5 (b), it is found that radial stress is approximately independent of the circumferential coordinate, especially in a long time.

Figures 6 (a) and (b) show the distribution of circumferential stress at various times and 3-D variations with respect to r and θ in time 1e4 sec, respectively. The magnitudes of circumferential stress are seen to increase with increasing time (Fig. 6a). It is also observed that, similar to radial stress, at long time. Changing circumferential stress along the θ coordinate is negligible.

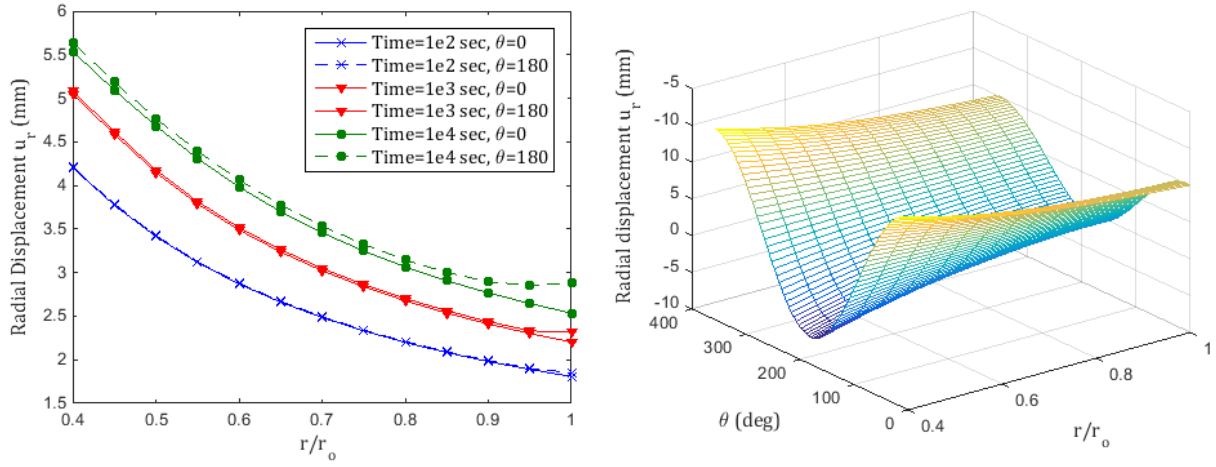

(a) (b)

Fig. 4. a) Radial distribution of radial displacement for different times and directions, b) 3-D distribution of the radial displacement for time 1e4 sec

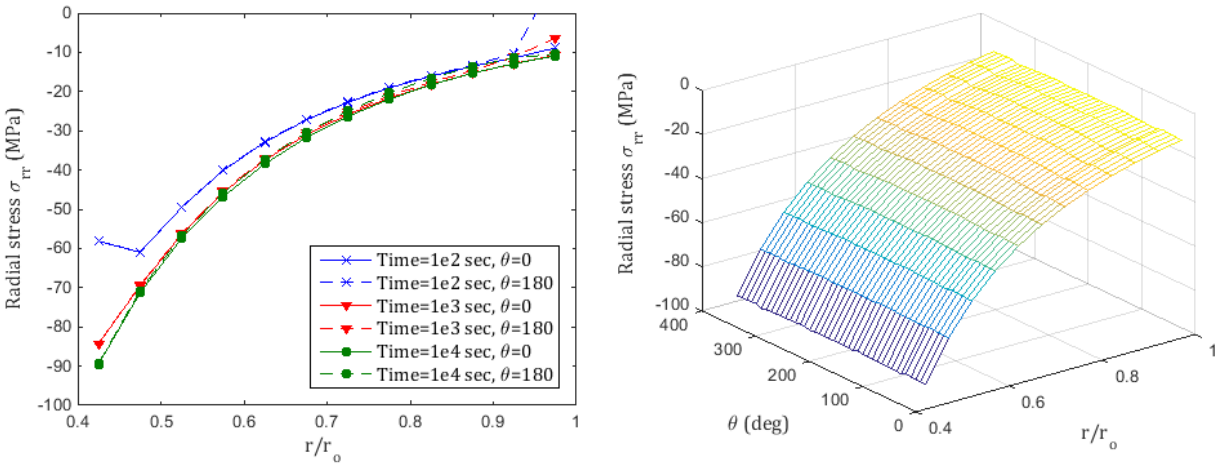

(a) (b)

Fig. 5. a) Radial distribution of radial stress for different times and directions, b) 3-D distribution of the radial stress for time 1e4 sec

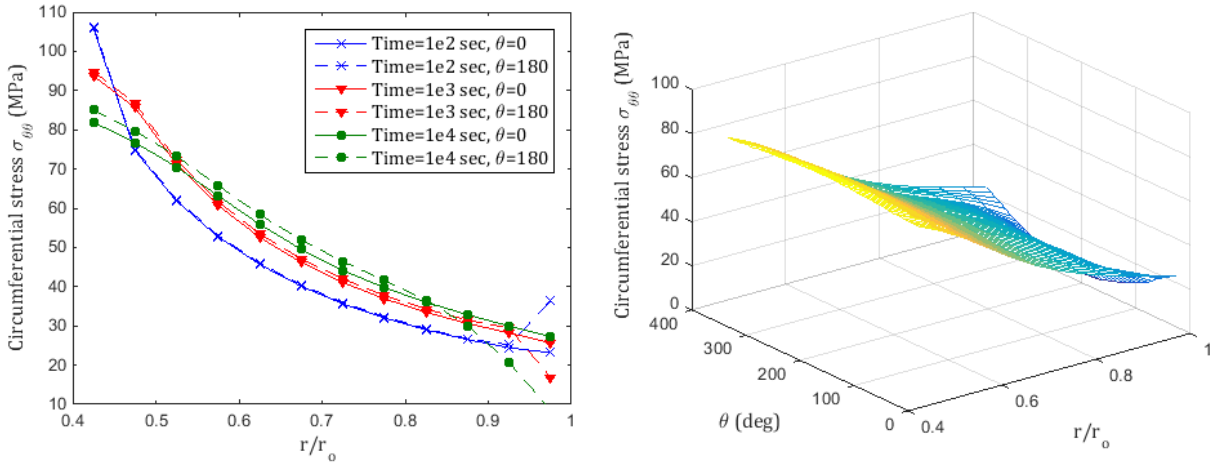

(a) (b)

Fig. 6. a) Radial distribution of circumferential stress for different times and directions, b) 3-D distribution of the circumferential stress for time 1e4 sec

As can be observed in Figures 5 and 6, radial and circumferential stresses are obtained approximately independent of θ coordinate. This can be justified by the magnitudes of thermal and mechanical boundary conditions, mentioned in Equation (28). In these loading conditions, the radial thermal gradient is considerably higher than circumferential thermal gradient. On the other hand, pressure gradient is applied radially and there is no pressure change in circumferential direction. Therefore, it can be observed that stress components are more dependent on radius than θ coordinate.

The radial variation in shear stress is shown in Figure 7 (a). It can be observed that at the same time, considerable difference exists between two directions θ=0 and 180. Indeed, the non-axisymmetric loads introduced in Equation (25) create significant shear stress in the structure. The 3-D distribution of shear stress in time 1e4 sec is presented in Figure 7(b). The strong dependency of shear stress to the circumferential direction can be observed in this figure.

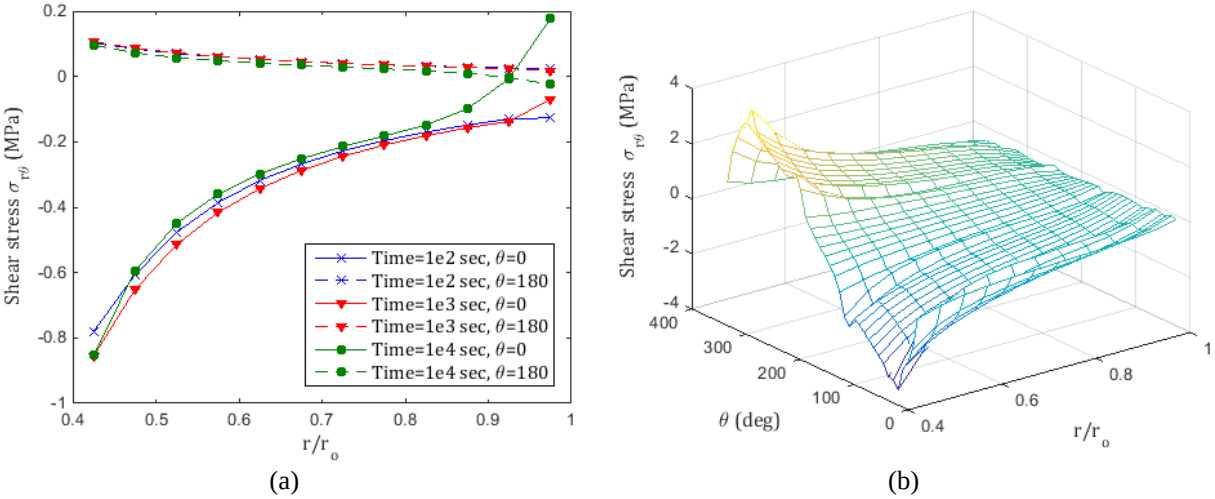

(a) (b)

Fig. 7. a) Radial distribution of shear stress for different times and directions, b) 3-D distribution of the shear stress for time 1e4 sec

To investigate structural damping effects of the viscoelastic material, time variations of radial and circumferential strain components for elastic and viscoelastic materials with same loading and geometrical conditions, are shown in Figure 8. It shows that for an elastic material, strain components tend to a constant value after some oscillations. However, in viscoelastic material, absolute magnitudes of the strain components are increased after fewer oscillations. From the comparison between elastic and viscoelastic materials, it is observed that viscoelastic materials have fewer oscillations and become smooth sooner than elastic materials.

4.2. Effect of inhomogeneities

In order to investigate the effects of radial and circumferential material inhomogeneities (m and n), the distribution of radial displacement and stress components along the radius in time 1000 sec are presented in the Figure 9, 10, 11 and 12. Due to the non-axisymmetric condition of the cylinder, the radial distribution of such parameters is shown for 4 directions: θ=0, 60, 120 and 180.

The distribution of radial displacement is presented in Figure 9. It is seen that, the displacement is increased with increasing radial and positive circumferential inhomogeneities. It can also be observed that the effect of radial inhomogeneity is major.

Figure 10 shows the variation in radial stress for different inhomogeneities. It is observed that changing values of m and n have no considerable effect on radial stress and the mechanical boundary conditions (internal and external pressures) are prevalent.

Figure 11 shows the distribution of circumferential stress. It can be concluded that increasing circumferential inhomogeneity to positive values, decreases circumferential stress throughout the radius and for negative inhomogeneities, circumferential stress becomes larger. On the other hand, increasing radial inhomogeneity, results in decreasing circumferential stress in the lower radii and an increase in upper radii. In fact, the radial dependency of the circumferential stress is decreased with increasing radial inhomogeneity.

According to the non-axisymmetric thermal boundary conditions, shear stress is created in the cylinder. Figure 12 illustrates the distribution of shear stress. It is observed that the variation in material inhomogeneity changes the magnitudes of shear stress, so that circumferential inhomogeneity has a major effect in the regard. It can be observed that a positive value of circumferential inhomogeneity decreases the absolute magnitude of shear stress. It is also observed that increasing radial inhomogeneity can reduce radial dependency of shear stress, smoothly.

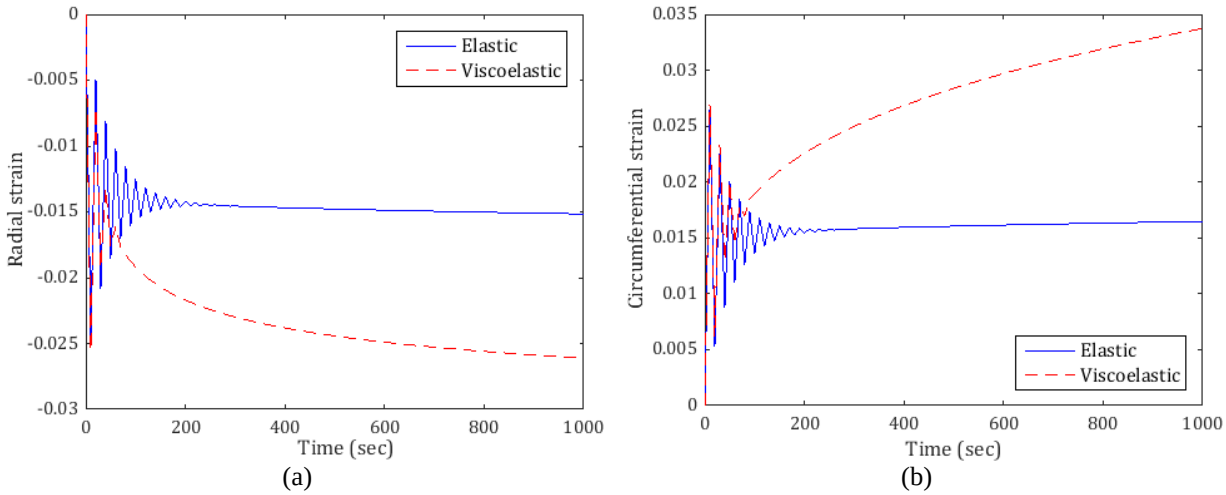

(a) (b)

Fig. 8. Time-dependent strain at (r,θ)=(0.35,0): a) Radial strain, b) circumferential strain

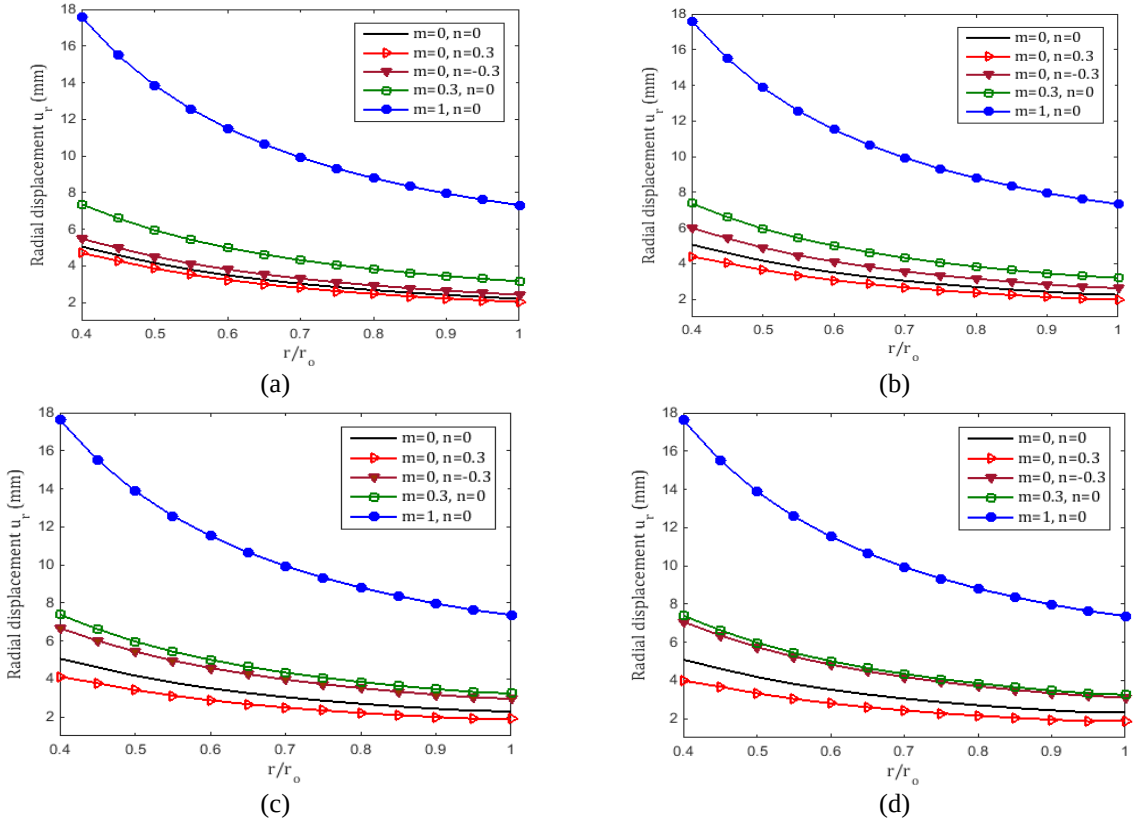

Fig. 9. Radial distribution of radial displacement in time=1e3 sec: a) $\theta = 0$, b) $\theta = 60$, c) $\theta = 120$, d) $\theta = 180$

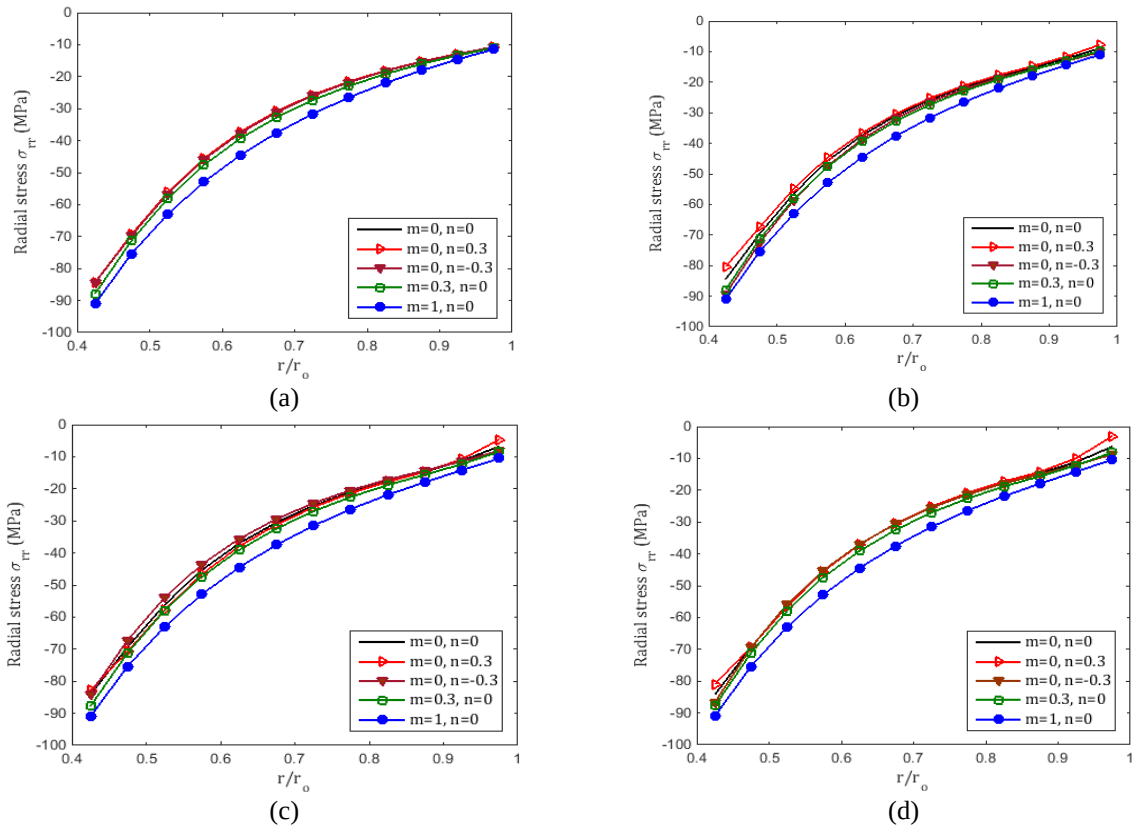

Fig. 10. Radial distribution of radial stress in time=1e3 sec: a) $\theta = 0$, b) $\theta = 60$, c) $\theta = 120$, d) $\theta = 180$

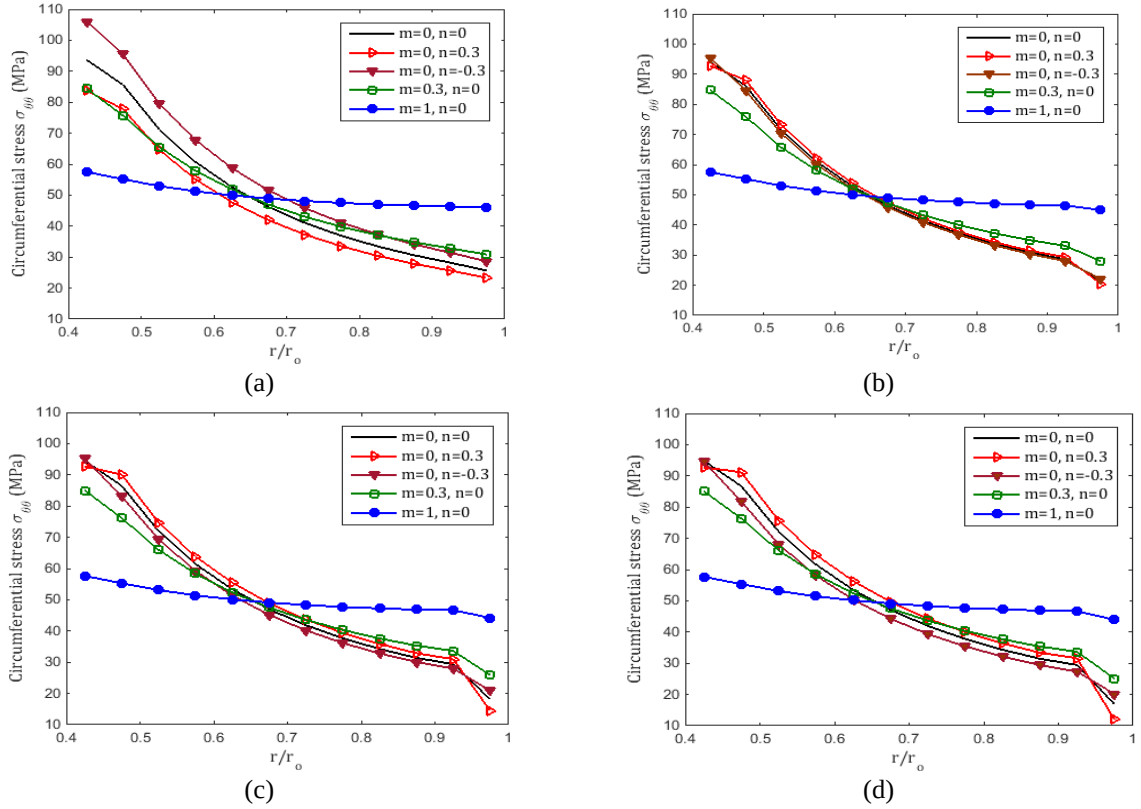

Fig. 11. Radial distribution of circumferential stress in time=1e3 sec: a) $= 0$, b) $\theta = 60$, c) $\theta = 120$, d) $\theta = 180$

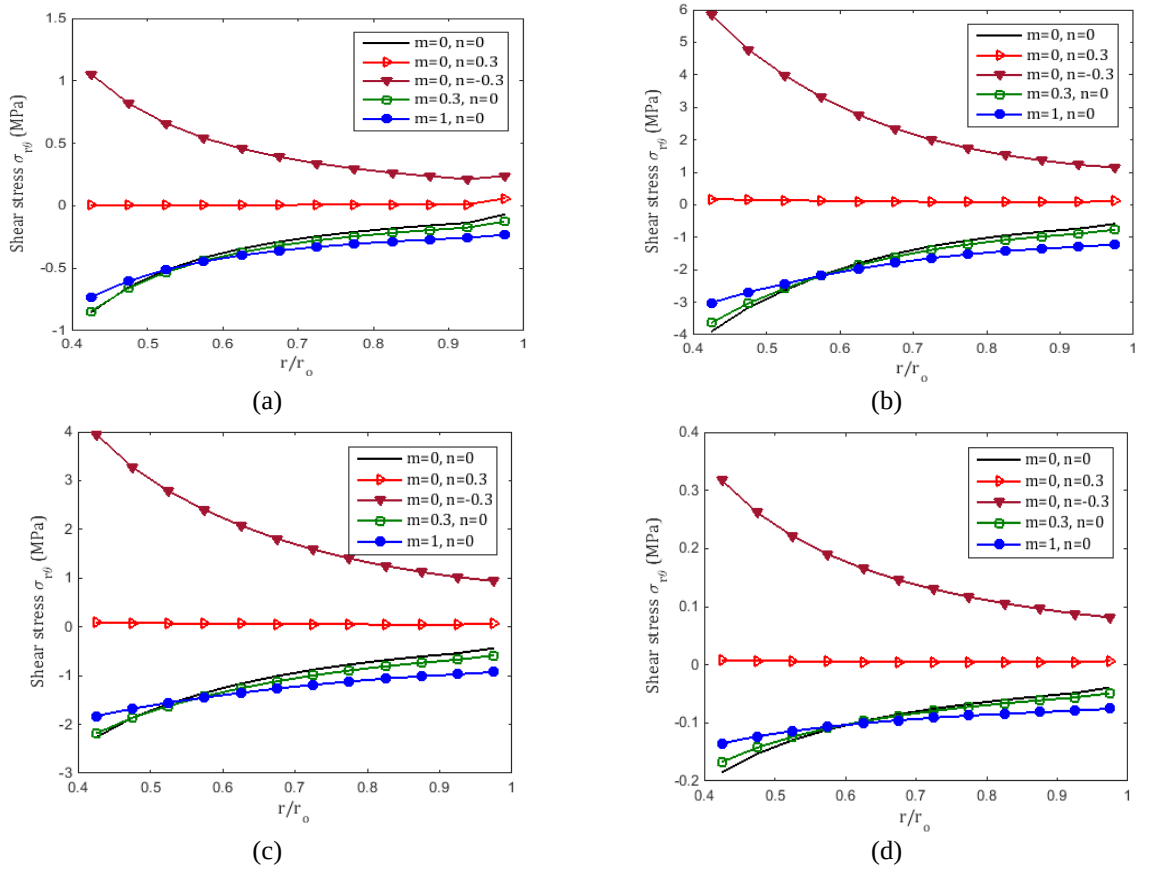

Fig. 12. Radial distribution of shear stress in time=1e3 sec: a) $= 0$, b) $\theta = 60$, c) $\theta = 120$, d) $\theta = 180$

4.3. Verification

To verify the results, the solution method presented in this study was applied on a problem of non-axisymmetric elastic response of a thick-walled cylinder investigated by Jabbari et al. [8]. They presented a cylinder with r_i=1 m and r_o= 1.2m, and the following thermal and mechanical boundary conditions were chosen as follows:

$$\begin{aligned} &T\left(r_i,\theta\right)=60\cos\cos 2\theta, T\left(r_o,\theta\right)=0 \\ &\sigma_{rr}\left(r_i,\theta\right)=0, \sigma_{r\theta}\left(r_i,\theta\right)=0 \\ &u_r\left(r_o,\theta\right)=0, u_\theta\left(r_o,\theta\right)=0 \end{aligned} \quad (30)$$

All the mechanical and thermal properties were assumed to be radially dependent as $P\left(r\right)=P_0 r^m$. The distribution of radial stress at $\theta=\pi/3$ is shown in Figure 13 (a). Agreement between results of this study with those obtained in Ref. [8] can be observed from this figure.

The time-dependent results corresponding to viscoelasticity can be compared with results of Guedes [25]. According to Guedes [25], a homogenous axisymmetric viscoelastic cylinder with 0.6 m and 0.8 m as inner and outer radii respectively, under 100 MPa and 40 MPa as inner and outer pressures, respectively is considered. The distributions of radial and circumferential stress in time 1e6 sec are illustrated in Figure 13 (b). It is observed that the time-dependent results are in agreement with Guedes [25].

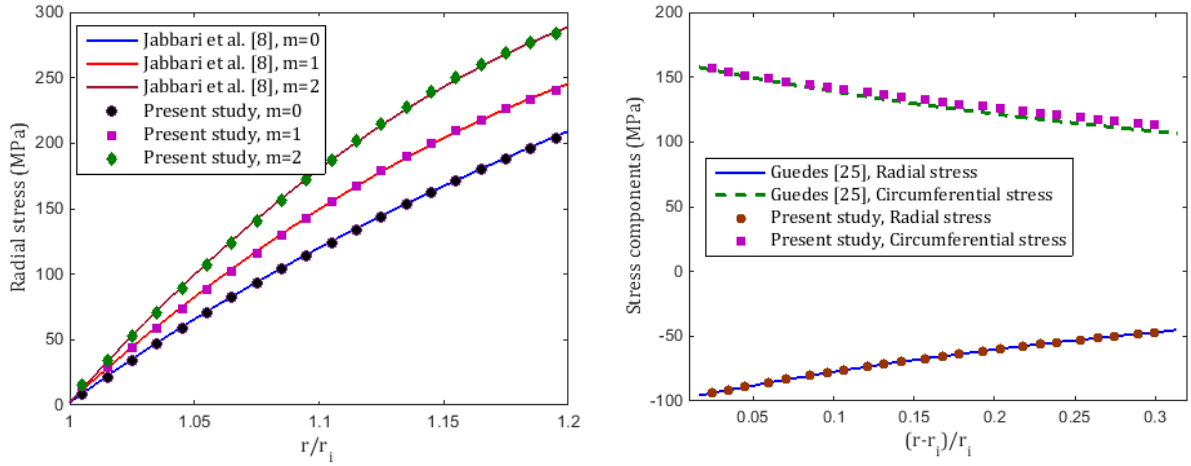

(a) (b)

Fig. 13. Verification of results: a) Distribution of radial stress for inhomogeneous elastic cylinder under non-axisymmetric loads, b) Distribution of radial and circumferential stresses for a homogenous viscoelastic cylinder

5. Conclusion

The transient thermoelasticity problem for non-axisymmetric cylinder, made of functionally graded viscoelastic materials is investigated in this research. The material is assumed to be radially and circumferentially nonhomogeneous. The comprehensive FE formulations of the problem considering all terms of balance and motion equations are derived. Results are presented for different times and various material inhomogeneities.

The following remarks can be concluded:

1. In homogenous material under non-axisymmetric loads, radial and circumferential stress components are approximately independent of the θ coordinate. While radial displacement and shear stress have significant variations with respect to θ.
2. Radial inhomogeneity has a considerable effect on displacement and circumferential stress. By increasing radial inhomogeneity, the displacement is increased and circumferential stress becomes radial-independent.
3. Circumferential inhomogeneity is much more effective on shear stress. Appropriate circumferential material inhomogeneity can reduce absolute values of shear stress, remarkably.

Reduction in stress components especially shear stress due to non-axisymmetric loads is

the most important issue for delaying failure and increasing the life of the structure. By using an appropriate radially and circumferentially inhomogeneous material proposed in this study, circumferential and shear stress can be controlled and decreased accordingly.

References

[1].Chen TC, Weng CI., 1989, Coupled transient thermoelastic response in an axi-symmetric circular cylinder by Laplace transform-finite element method. Comput Struct 33(2): 533-542.

[2].Lee ZY., 2006, Generalized coupled transient thermoelastic problem of multilayered hollow cylinder with hybrid boundary conditions. Int Commun Heat Mass 33(4): 518–528.

[3].Chitikireddy R, Datta SK, Shah AH, Bai H., 2011, Transient thermoelastic waves in an anisotropic hollow cylinder due to localized heating. Int J Solids Struct 48(21): 3063–3074.

[4].Jabbari M, Bahtui A, Eslami MR., 2009, Axisymmetric mechanical and thermal stresses in thick short length FGM cylinders. Int J Pres Ves Pip 86(5): 296–306.

[5].Ying J, Wang HM., 2010, Axisymmetric thermoelastic analysis in a finite hollow cylinder due to nonuniform thermal shock. Int J Pres Ves Pip 87(12): 714–720.

[6].Sadd M., 2005, Elasticity, theory, applications and numeric. Elsevier, Kingston Elsevier.

[7].Takeut Y, Nod N., 1980, Three-dimensional transient thermal stresses in a finite circular cylinder under nonaxisymmetric temperature distribution. J Therm Stresses 3(2): 159-183.

[8].Jabbari M, Sohrabpour S, Eslami MR., 2003, General Solution for Mechanical and Thermal Stresses in a Functionally Graded Hollow Cylinder due to Nonaxisymmetric Steady-State Loads. J Appl Mech 70(1): 111–118.

[9].Tokovyy YV, Ma CC., 2008, Analysis of 2D non-axisymmetric elasticity and thermoelasticity problems for radially inhomogeneous hollow cylinders. J Eeg Math 61(2-4): 171-184.

[10]. Tokovyy YV, Ma CC., 2009, Analytical solutions to the planar non-axisymmetric elasticity and thermoelasticity problems for homogeneous and inhomogeneous annular domains. Int J Eng Sci 47(3): 413–437.

[11]. Li H, Liu Y., 2014, Functionally graded hollow cylinders with arbitrary varying material properties under nonaxisymmetric loads. Mech Res Commun 55: 1–9.

[12]. Zheng BJ., Gao XW., Yang K., Zeng C., A novel meshless local Petrov–Galerkin method for dynamic coupled thermoelasticity analysis under thermal and mechanical shock loading. Eng Anal Bound Elem, doi:10.1016/j.enganabound.2014.12.001, in press.

[13]. Jin ZH., 2006, Some Notes on the Linear Viscoelasticity of Functionally Graded Materials. Math Mech Solids 11(2): 216–224.

[14]. Zhang NH, Wang ML., 2007, Thermoviscoelastic deformations of functionally graded thin plates. Eur J Mech A-Solid 26(5): 872–886.

[15]. Altenbach H., Eremeyev VA., 2008, Analysis of the viscoelastic behavior of plates made of functionally graded materials. J Appl Math Mech-Uss 88(5): 332–341.

[16]. Chen SS, Xu CJ, Tong GS., 2015, A meshless local natural neighbour interpolation method to modeling of functionally graded viscoelastic materials. Eng Anal Bound Elem 52: 92–98.

[17]. Temel B, Yildirim S, Tutuncu N., Elastic and viscoelastic response of heterogeneous annular structures under Arbitrary Transient Pressure. Int J Mech Sci, doi: 10.1016/j.ijmecsci.2014.08.021, in press.

[18]. Lakes R., 2009, Viscoelastic materials, Cambridge University Press, New York.

[19]. Moreau S., Chrysochoos A., Muracciole JM., Wattrisse B., 2005, Analysis of thermoelastic effects accompanying the deformation of PMMA and PC polymers. Comptes Rendus Mécanique, 333(8): 648-653.

[20]. Volodin VP., Slutsker, AI., 1994, Specific features of the thermoelastic effect in polymers. Thermochimica acta, 247(1): 121-128.

[21]. Hetnarski R, Eslami MR., 2008 Thermal stresses – Advanced theory and applications, Springer, New York.

[22]. Payette GS, Reddy JN., 2010, Nonlinear quasi-static finite element formulations for viscoelastic Euler–Bernoulli and Timoshenko beams. Int J Numer Method Biomed Eng 26(12): 1736–1755.

[23]. Luche J, Rogaume T, Guillaume E., 2011, Characterization of thermal properties and analysis of combustion behavior of PMMA in a cone calorimeter. Fire Safety J 46(7): 451-461.

[24]. Ashby MF., 2005 Materials selection in mechanical design, Elsevier, Cambridge.

[25]. Guedes RM., 2010, Nonlinear viscoelastic analysis of thick-walled cylindrical composite pipes. Int J Mech Sci 52(8): 1064–1073.